Available online at www.sciencedirect.com
SCIENCE DIRECT
Journal of Photochemistry and Photobiology A: Chemistry 179 (2006) 298–304
Journal of Photochemistry and Photobiology A:Chemistry
www.elsevier.com/locate/jphotochem

A butterfly like motion as a clue to the photophysics of thioxanthone

Òscar Rubio-Pons [a], Luis Serrano-Andrés [b,*], Dominique Burget [c], Patrice Jacques [c]

[a] *Department of Biotechnology, Royal Institute of Technology, Albanova University Center, Roslagstullsbacken 15, SE-106 91 Stockholm, Sweden*
[b] *Instituto de Ciencia Molecular, Universitat de València, Dr. Moliner 50, Burjassot, ES-46100 Valencia, Spain*
[c] *Department of Photochemistry, Université de Haute-Alsace, E.N.S.C.Mu, 3 rue Alfred Werner, F-68093 Mulhouse Cedex, France*

Received 19 July 2005; received in revised form 21 August 2005; accepted 25 August 2005
Available online 26 September 2005

Abstract

A theoretical, quantum-chemical study of the thioxanthone (TX) molecule has been performed at the MP2 and CASPT2 levels of theory. Geometries, absorption energies, and transition and state properties have been investigated. Two conformers have been found very close in energy with planar (P) and non-planar (NP) structures, the latter characterized by a dihedral angle $\theta = 173.3^\circ$ representing the bend of the side benzene rings and an out-of-plane angle $\phi = 4^\circ$ of the C=O bond. Large changes in the relative positions and properties of the two low-lying electronic absorption bands, $\pi\pi^*$ and $n\pi^*$, are computed when changing the conformation. As a consequence of the analysis of the TX absorption spectrum it is suggested that TX should be viewed as dynamically changing its conformation between the planar and the non-planar conformations. We coined such behavior as a "butterfly like motion". This dynamic view of the TX structure enables a plausible explanation of the photophysical properties observed for the system.

Keywords: Thioxanthone; Absorption spectrum; CASPT2; Ground state structure

1. Introduction

Thioxanthone (TX) has been used as an example of the photophysical manifestations of vibronic coupling between nearby $n\pi^*$ and $\pi\pi^*$ excited states. Its fluorescence quantum yield (ϕ_F) increases from 0.00062 in THF to 0.23 in ethylene glycol [1,2]. This dramatic solvent effect was attributed to the decrease of the $S_1(\pi\pi^*) \rightarrow S_0$ internal conversion rate [3] because of the vibronic perturbation of the $S_1(\pi\pi^*)$ state by the close-lying ($n\pi^*$) state (phenomenon termed "proximity effect" [3]). Indeed, as the polarity increases, the vibronic perturbation of $S_1(\pi\pi^*)$ by the close-lying electronic state $S_2(n\pi^*)$ decreases, since S_2 is destabilized compared to S_1 [1] (see Scheme 1). Alternatively, the fluorescence quenching could be also due to the presence of a conical intersection S_1/S_0 less accessible in polar solvents. From Table 1 it can be observed that the fluorescence lifetime (τ_F) [2] and the triplet quantum yield ϕ_T [4] are also strongly solvent dependent. Curiously, apart from cursory investigations based on PPP [5] and CNDO/S [6] calculations, no detailed interpretation of the TX absorption spectrum was reported in the literature.

Considering that even the basic features of the photophysics of TX were unresolved, we undertook the project of studying its low-lying excited states with a high-quality quantum-chemical method like the CASPT2 procedure, a powerful theoretical approach that has proved its accuracy by now [7–10]. In the present paper, geometries of ground and excited states minima, transition energies and state properties will be presented in order to give insight to some of the basic photophysical characteristics of TX as an isolated system.

2. Computational details

Several methods and basis sets were employed to optimize the ground state geometry of the TX molecule (see Fig. 1), as explained in the following section. Finally, geometries obtained at the highest employed level, MP2/6-31G(d), were used to compute excited states and ionization potentials in both C_{2v} planar (P) and C_s non-planar (NP) conformers (there are two symmetric non-planar conformers called NP and −NP). The C_s structure has the symmetry plane intersecting the molecule by the S–C_c=O axis (see Fig. 2). In this way the coplanarity

* Corresponding author. Tel.: +34 963544333; fax: +34 963543156.
E-mail address: Luis.Serrano@uv.es (L. Serrano-Andrés).

1010-6030/$ – see front matter © 2005 Elsevier B.V. All rights reserved.
doi:10.1016/j.jphotochem.2005.08.033

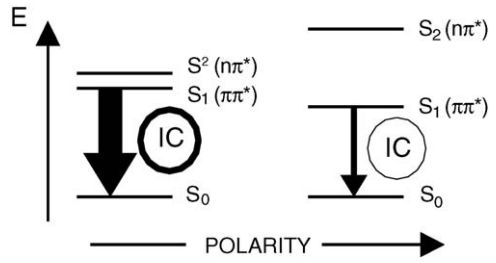

Scheme 1. Changes in the internal conversion (IC) efficiency due to the "proximity effect" in thioxanthone.

Table 1
Dependence of thioxanthone photophysical characteristics on solvent polarity

Solvent	τ_F (ns) [1,2]	Φ_F ($\times 10^3$) [1,2]	Φ_T [4]
Cyclohexane			~0.85
THF		0.62	
Ethylacetate			~0.80
Acetonitrile	0.07	4.1	0.66
Methanol	2.55	120	0.56
Ethylene glycol	4.6	230	

of the two aromatic rings might be broken. The interchange between the three conformers of TX (NP to P and to −NP) leads to the mentioned "butterfly motion". Optimization of the P conformer directly led to a C_{2v} structure. To compute excited states, the Complete Active Space (CAS) SCF multiconfigurational method, complemented by the second-order perturbative approach, CASPT2, was employed. [11]. The active space used in the selection of the multiconfigurational reference was 13 active orbitals and 12 electrons, including the oxygen lone pair and 11 $\pi\pi^*$ orbitals, and it was selected by careful analysis of the natural occupation numbers of the orbitals obtained in control Restricted Active Space (RAS) SCF calculations [12]. An accurate one-electron basis set was employed: Atomic Natural Orbitals (ANO-L) contracted to S 5s4p2d/C,O 4s3p1d/H 2s1p [13] in the fixed nuclei calculations. Gaussian '98 [14] and Molcas 6 [15] programs were used.

3. Results and discussion

3.1. Ground state structure

Gas-phase electron diffraction [16] and calorimetry [17] studies on TX suggest that the molecule has a slightly non-planar ground state structure. In particular, the dihedral angle between the two benzene rings has been measured $\Theta = 169.0 \pm 1.6°$ (angle $C_6C_5SC_{5'}$, see Fig. 1) [16]. Different semiempirical (AM1), density functional (B3LYP/6-31G(d)), and ab initio (HF/6-31G(d), RASSCF/ANO) geometry optimizations favored instead a planar, C_{2v} structure for TX. Such conformation was adopted for computing the ionization potentials within the HMO, MINDO/3, MNDO, PM3 [18], and DFT (B3LYP) methods [19], and the static polarizability using the coupled perturbed Hartree–Fock (CPHF) approach [20]. A correlated ab initio method like MP2/6-31G(d) yielded however a slightly non-planar geometry for TX, with a computed dihedral angle $\Theta = 173.3°$. The sulfur and the carbonyl group form the axis of a bent molecule in which the C_s symmetry is kept. Undoubtedly, the presence of the sulfur atom in the molecular skeleton and the large S–C_5 bond lengths yield a flexible ring structure which favors non-planar conformations, as observed in thianthrene, where the carbonyl group is substituted by another sulfur atom and the dihedral angle reaches 128.1° [16].

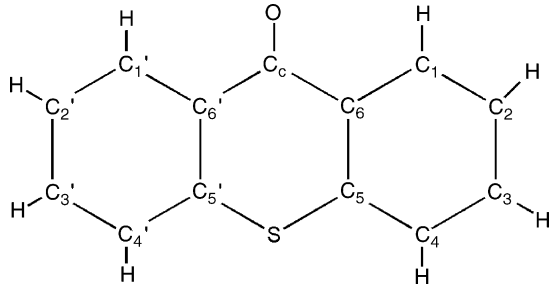

Fig. 1. Thioxanthone structure and atom labelling.

For the sake of comparison, two geometries will be employed in the present paper for the TX ground state minima: the mentioned non-planar MP2/6-31G(d) geometry (hereafter NP, with a symmetric corresponding −NP conformation), and a planar MP2/6-31G(d) structure in which planarity has been imposed (hereafter P) (Fig. 2). The non-planar structure is more stable (thermally corrected enthalpies) by 0.6 kcal/mol, and has a low-frequency vibration mode at 12.2 cm^{-1} (computed at the same level within the harmonic approach) corresponding to out-of-plane displacements of the S–C_c=O atoms. The same mode has an imaginary frequency of 9.7i cm^{-1} in the planar structure. It is therefore clear that the potential energy surface for the ground state will be extremely flat in this region. Table 2 compiles the computed theoretical results for both structures together with the data recorded by electron diffraction. Good agreement

Table 2
Main structural parameters for the ground state of thioxanthone

Parameter[a]	Theoretical[b]		Experimental[c]
	P	NP	
$r(C_1–C_2)$ (Å)	1.386	1.386	1.401[d]
$r(C_2–C_3)$ (Å)	1.403	1.403	1.401[d]
$r(C_3–C_4)$ (Å)	1.386	1.386	1.401[d]
$r(C_4–C_5)$ (Å)	1.407	1.407	1.401[d]
$r(C_5–C_6)$ (Å)	1.406	1.406	1.401[d]
$r(C_6–C_1)$ (Å)	1.408	1.408	1.401[d]
r(C–H) (Å)	1.087[d]	1.087[d]	1.099[d]
$r(C_5–S)$ (Å)	1.754	1.754	1.751
$r(C_6–C_C)$ (Å)	1.483	1.483	1.498
$r(C_C–O)$ (Å)	1.239	1.239	1.232
$\angle(C_5SC_{5'})$ (°)	103.3	103.1	103.4
Dihedral angle, Θ ($C_5C_6SC_{5'}$) (°)	0.0	173.3	169.0
Out-of-plane C_c=O angle, ϕ (°)	0.0	4.1	–

[a] Molecular symmetry: C_s (NP) and C_{2v} (P). The vertical symmetry plane contains the axis S–C_c–O.
[b] Fully optimized MP2/6-31G(d) non-planar (NP) and planarity restricted (P) MP2/6-31G(d) structures.
[c] Electron diffraction measurements [16].
[d] Average values.

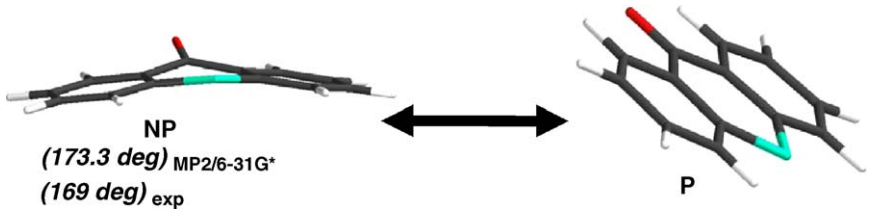

Fig. 2. P and NP structures of thioxanthone.

can be observed between the theoretical and the experimental [16] results, with a largest deviation, 0.015 Å, found for the C_c–C_6 bond length. The differences between the computed bond lengths of the C_{2v} P and the C_s NP structures are also minimal. Most importantly, the computed value of the dihedral angle Θ of the NP conformer is close to the experimental value. As a matter of fact, and considering that the difference in stability between both structures is lower than the thermal limit, we propose here that many physical features of TX can be nicely explained if (and only if) planar and non-planar conformations are taken into account in variable proportion.

Surprisingly, despite the small differences found in geometries for both structures, the electronic properties of the molecule are significantly affected by the change in conformation, undoubtedly due to the changes in conjugation of the π cloud. Table 3 compiles the theoretical (CASPT2/ANO) and experimental [18,19] ionization potentials (IP) for TX. The computed results correspond to vertical ionization potentials for TX obtained as differences between the neutral ground state molecule and the states of the TX cations at the geometry of the neutral ground state, planar (P) and non-planar (NP). There is an overall agreement between the computed and the experimental data, and in particular the correlation is better for non-planar TX (see Fig. 3). Considering the structure of TX as a combination of planar and non-planar conformations, it is not surprising than the latter better represents the measured data, since the photoelectron spectrum is recorded at high temperatures [18,19] which are expected to favor population of non-planar structures.

3.2. *Visible absorption spectrum and relative positions of the ππ* and nπ* states*

Breaking the planarity has even more striking consequences for the absorption spectrum of TX. For the sake of clarity, it is convenient to discuss separately the low energy part of the absorption spectrum (range 320–420 nm) from the higher energy region, which will be discussed in the next subsection. Indeed, from the photophysical point of view, the former is the region of interest since the proximity effect invoked for explaining the dramatical variation of the fluorescence quantum yield (ϕ_f) is based on the two transitions ($\pi\pi^*$) and ($n\pi^*$) located in this region. Table 4 compiles the theoretical excitation energies and excited state properties of TX at the ground state planar and non-planar conformations and compare the results with the experimental absorption spectrum in cyclohexane [1] since the gas phase spectrum is not available (cf. Fig. 4). The calculations were performed at the CASPT2/ANO//MP2/6-31G(d) level of theory. Focusing on the 320–420 nm region, only two transitions are computed in both conformers: (i) one of $\pi\pi^*$ type with moderate intensity attributed in part to a charge transfer like transition from the sulfur atom to the carbonyl group and in part to a variation of the electronic density in the π cloud upon excitation (see Fig. 5), and (ii) one of $n\pi^*$ type, therefore a forbidden transition which implies mainly the carbonyl group and the benzene ring. These descriptions are based on computed charge density difference plots between the ground and the excited states displayed in Fig. 5, which inform about the variation of the electronic density upon excitation. The charge density shifts are similar for the two low-lying transitions in both conformers. There is however a noticeable larger charge withdrawing from the sulfur atom in

Table 3
Comparison of the vertical ionization potentials (IPs, eV) of the planar (P) and non-planar (NP) conformations of thioxanthone with the experimental data

Theoretical (CASPT2)		Experimental	
P	NP	Ref. [18]	Ref. [19]
7.69 (π_1)	7.84 (π_1)	8.04	7.94 peak
8.84 (n_O)	9.03 (n_O)	9.12	9.0 shoulder
8.94 (π_2)	9.14 (π_2)	9.34	9.29 peak
9.19 (π_3)	9.17 (π_3)		
9.21 (π_4)	9.60 (π_4)		9.5 shoulder
			9.7 shoulder
10.32 (π_5)	10.97 (π_5)	10.87	10.8 peak

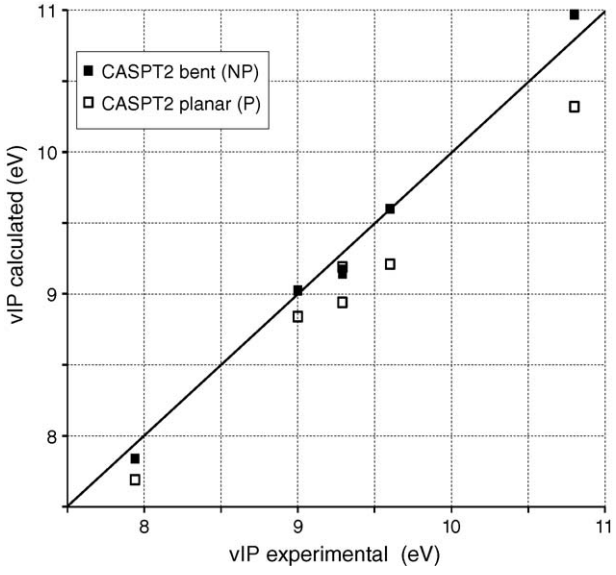

Fig. 3. Comparison of the computed vertical ionization potentials (vIP) of the planar (P) and non-planar (NP) conformation with experimental data [18,19].

Table 4
Computed (conformers P and NP) and experimental (cyclohexane [1]) excitation energies (ΔE, eV), wavelengths (λ, nm), oscillator strengths (f), and dipole moments (μ, D) of thioxanthone

State	P (C_{2v})				State	NP (C_s)				Experimental	
	CASPT2		CAS			CASPT2		CAS		λ (nm)	ΔE (eV)
	λ (nm)	ΔE (eV)	f	μ		λ (nm)	ΔE (eV)	f	μ		
1^1A_1				1.69[a]	$1^1A'$				2.22[a]		
$2^1A_1(\pi\pi^*)$	387	3.20	0.098	5.92	$1^1A''(n_O\pi^*)$	355	3.49	0.000	0.80	377	3.29
$1^1A_2(n_O\pi^*)$	336	3.69	0.000	−0.02	$2^1A'(\pi\pi^*)$	345	3.59	0.070	2.79	362	3.43
$1^1B_2(\pi\pi^*)$	306	4.05	0.131	2.81	$2^1A''(\pi\pi^*)$	301	4.12	0.040	4.01	298	4.16
$3^1A_1(\pi\pi^*)$	283	4.38	0.104	3.16	$3^1A'(\pi\pi^*)$	275	4.51	0.140	3.51	287	4.32
$2^1B_2(\pi\pi^*)$	274	4.52	0.020	2.00						274 sh	4.53
$4^1A_1(\pi\pi^*)$	264	4.70	0.002	4.13						267 sh	4.64
$3^1B_2(\pi\pi^*)$	258	4.80	0.918	2.85	$3^1A''(\pi\pi^*)$	259	4.79	0.342	7.49	256	4.84
					$4^1A''(\pi\pi^*)$	248	5.00	0.012	1.30	247 sh	5.02
$5^1A_1(\pi\pi^*)$	241	5.14	0.014	3.69	$4^1A'(\pi\pi^*)$	240	5.17	0.112	7.44		
$1^1B_1(n\pi^*)$	239	5.19	0.001	−0.57							
$4^1B_2(\pi\pi^*)$	234	5.30	0.012	2.47							
$5^1B_2(\pi\pi^*)$	223	5.56	0.302	2.14						222	5.58
$2^1A_2(n\pi^*)$	215	5.77	0.000	−0.40							
$6^1A_1(\pi\pi^*)$	214	5.79	0.021	2.68						218 sh	5.69

[a] Ground state dipole moment in benzene, 2.65 D [21].

the non-planar forms (probably due to a decrease in the π conjugation in the molecule) in particular for the lowest-energy $n\pi^*$ transition.

A noticeable fact is that a slight deviation from planarity induces very large changes in the transition energies, dipole moments, and, more importantly, on the relative positions of the two transitions. All these aspects deserve now a detailed discussion. For the planar structure, the allowed $S_0 \rightarrow S_1(\pi\pi^*)$ transition of P (2^1A_1) computed at 387 nm (3.20 eV) can be easily related to the maximum of the experimental spectrum in this region, $\lambda = 377$ nm (3.29 eV). However, the forbidden $S_0 \rightarrow S_2(n_O\pi^*)$ transition of P (1^1A_2, not observed in the spectrum) is computed higher in energy by 0.5 eV. The upper position of the $n_O\pi^*$ transition compared to $\pi\pi^*$ transition is in agreement with Scheme 1 but it is crucial to realize that the 0.5 eV gap is too large for an efficient mixing of the two transitions. Quite interestingly, the excited states relative positions changes for the non-planar conformer. The allowed $S_0 \rightarrow S_2(\pi\pi^*)$ transition of NP ($2^1A'$) is calculated at 345 nm (3.60 eV) and corresponds roughly to the shoulder observed at 362 nm (3.43 eV). Therefore, the profile of the lowest-energy band can be basically described by taking into account out-of-plane vibrational progressions of the lowest $\pi\pi^*$ electronic transition (Scheme 2). The forbidden $S_0 \rightarrow S_1(n_O\pi^*)$ excitation of NP ($1^1A''$) (again not observed in the spectrum) is computed here lower in energy by 0.1 eV. Now, the energy gap is by far more favorable to the vibronic perturbation of $S_1(\pi\pi^*)$ by the close lying $S_2(n\pi^*)$. However,

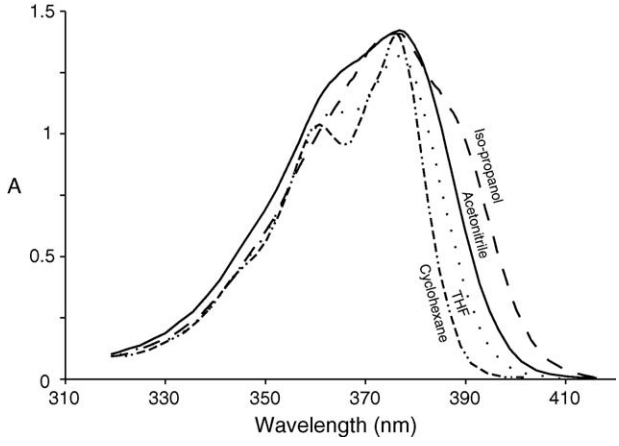

Fig. 4. Visible absorption spectrum of thioxanthone in solvents of representative polarities [1].

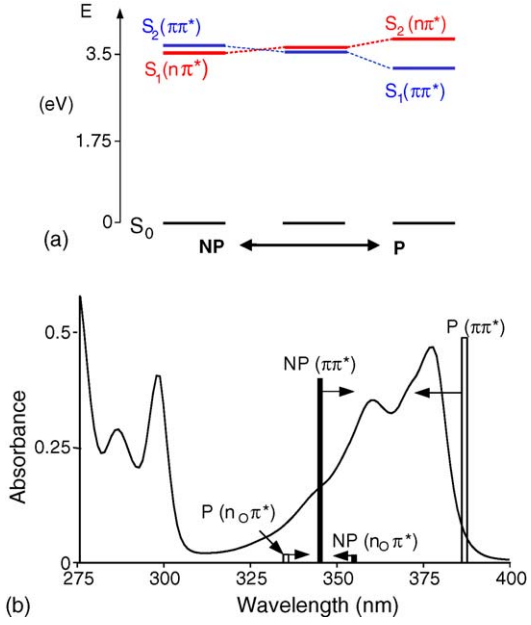

Scheme 2. (a) Calculated energy diagram of the N and NP limit conformers compared to the "proximity effect" as reported in Scheme 1. (b) Fitting of the UV absorption spectrum in cyclohexane with the calculated transitions of the NP and P conformers.

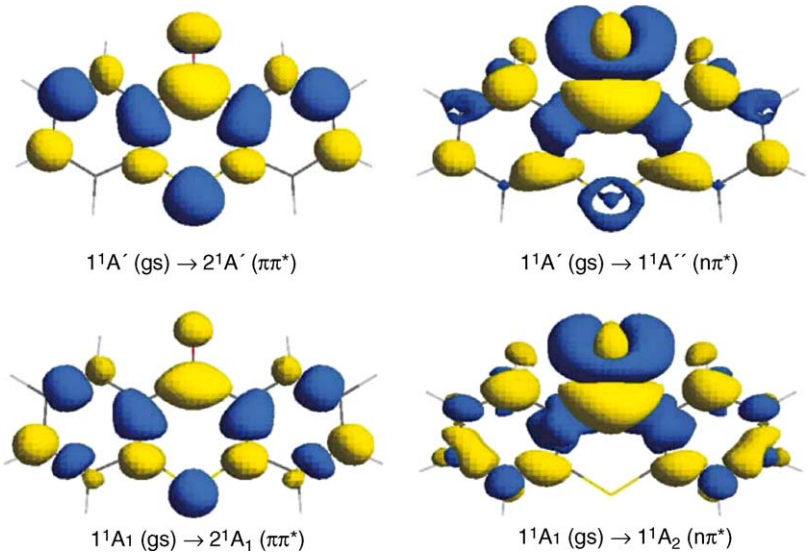

Fig. 5. Differential electron density (CASSCF) for the two low-lying singlet–singlet valence transitions in thioxanthone computed at the ground state non-planar (NP, C_s, top) and planar (P, C_{2v}, bottom) optimized geometries. The electron density is shifted upon light-induced excitation from darker to lighter regions.

the relative position of S_1 and S_2 is now in contradiction with Scheme 1.

It appears consequently that these two important items, visible absorption spectrum and "proximity effect", cannot be both correctly described from a single conformation: P or NP conformers reported in Table 4. However, these two structures correspond to a static vision of the molecule. Indeed, it is clear from the quasi-energetic degeneracy of P and NP conformations that they are only "limit" situations. It is the originality of the present work to propose that there is in reality a continuous interchange of the conformations P ↔ NP (or P ↔ −NP) in which the molecule adopts, preferably, non-planar structures. This phenomenon can be well described by the term "butterfly like motion". Thus, the experimental properties of TX corresponds to a dynamic vision of the molecule, i.e., to the continuous change of the conformation. Quite evidently, it is illusive to look for a quantitative description of the real situation. However, it is remarkable that a thorough comprehension of both the proximity effect and the visible spectrum is now accessible since the experimental data is surrounded by the two limit theoretical data associated to the P and NP conformers as tentatively illustrated in Scheme 2.

3.3. UV absorption spectrum

Table 4 lists the computed properties for the low-lying excited states of TX up to 214 nm, together with transitions and state properties and comparison with the experimental absorption spectrum in cyclohexane [1]. Fig. 6 displays graphically the experimental spectrum together with the computed features. The absorption spectrum of TX shows, up to 210 nm, four basic band systems. With regards to the assignment of the observed bands, it has been already discussed how the lowest-energy band ranging from 380 to 340 nm contains two transitions to the lowest $\pi\pi^*$ and $n\pi^*$ singlet states. The intensity of the band must be attributed to the more intense $\pi\pi^*$ transition, while the $n\pi^*$ band is surely obscured beneath. Considering the results for both conformers, the peaks observed at 377 nm (3.29 eV) and 362 nm (3.43 eV) can be attributed to the transition to the $\pi\pi^*$ state in its planar and non-planar structures. The final profile of the band will be a consequence of the vibrational progressions, specially those related with the bending, out-of-plane mode.

The second band system includes two medium intensity maxima at 298 nm (4.16 eV) and 287 nm (4.32 eV) and a couple of shoulders at 274 nm (4.53 eV) and 267 nm (4.64 eV) placed in the low-energy tail of the most intense band of the spectrum. Several $\pi\pi^*$ transitions have been computed in this region. The bands at 4.16 and 4.32 eV can be assigned to the transitions to the $2^1A''$ (1^1B_2) and $3^1A'$ (3^1A_1) $\pi\pi^*$ states, computed at 4.12 (4.05) and 4.51 (4.38) eV for the NP and P conformers, respec-

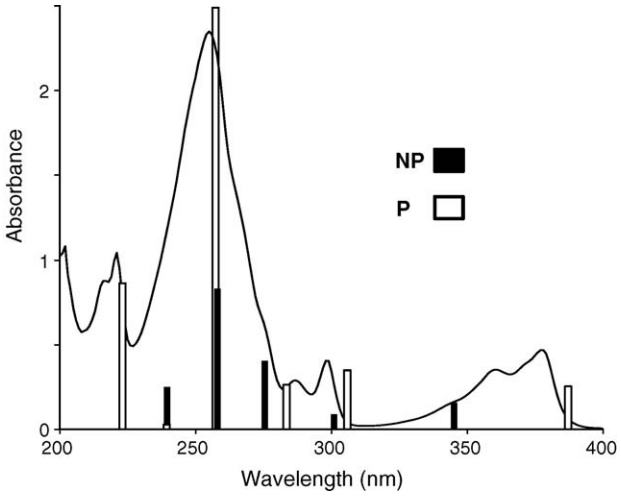

Fig. 6. Thioxanthone absorption spectra in cyclohexane [1]. CASPT2 transitions for the planar (P) and non-planar (NP) conformations studied also included.

tively, and with intermediate oscillator strengths (from 0.040 to 0.140). The nature of the transition to the $2^1A''$ (1^1B_2) state is similar to that of the lowest $\pi\pi^*$ state: the charge is basically transferred from the sulfur to the carbonyl group (with a consequent increase in the dipole moment) and redistributed within the benzene rings. Regarding the mentioned shoulders, they better match two low-intensity transitions computed at 4.52 and 4.79 eV in the planar conformer. Surprisingly, these two transitions seem to be pushed to higher energies in the non-planar form. It is clear, in any case, that the next transition, computed to the 3^1B_2 (P) or $3^1A''$ (NP) $\pi\pi^*$ states at 258 nm (4.80 eV) and 259 nm (4.79 eV) with large oscillator strengths, 0.918 and 0.342, respectively, is perfectly related to the most intense band in the spectrum at 256 nm (4.84 eV), which proves to be almost insensitive to the bending of the ground state. From the higher transitions, just to mention the intensity (0.302) of the computed 223 nm (5.56 eV) band, which explains the presence of the 222 nm (5.56 eV) recorded peak. We want to point out that, because of the lower symmetry, calculations on the NP C_s conformer become more difficult, and the number of computed states has to be reduced in comparison to the P C_{2v} calculations.

3.4. Dipole moments

Regarding the dipole moments of the computed states, values of 1.69 and 2.22 Debyes (D) are obtained for the ground state of TX in its P and NP forms, respectively, at the CASSCF level of calculation. Changing the level of the theory to MP2 the values increase by near 0.2 D. The ground state dipole moment was reported $\mu_g^{exp} = 2.65$ D in benzene [21]. The value in gas phase is unknown but should be somewhat lower. Applying the dynamical view of the TX conformation the expected value for the dipole moment would be intermediate between both structures, near 2 D. Dipole moments for the low-lying excited states of TX considerably differ in its P and NP conformers. Differences $\Delta\mu(P) = +4.2$ D and $\Delta\mu(NP) = +0.6$ D have been computed at the CASSCF level. Within the previous approximation, one's would expect an intermediate value of about $\mu_{ex} - \mu_g = +2.4$ D which is close to an experimental value of $\Delta\mu = +2.65$ D reported by Abdhullah and Kemp [22]. However, it can be easily seen that the overall evolution of the absorption spectrum with increasing solvent polarity is not at all straightforward to interpret (Fig. 4) which precludes any quantitative comparison.

It is probably the balance between both conformations which is the responsible for the ultimate photophysical properties of TX in solution. This phenomenon in which the measured absorption spectrum in different solvents depends dynamically on different structures was already proposed in the case of molecular tautomers, for instance in adenine [23] and benzotriazole [24]. We are reluctant to propose a more detailed explanation of the computed values at the view of the solvatochromic behavior of TX. A change of the solvent would certainly affect the characteristic of the limit conformers P and NP as well as the dynamical interconversion P ↔ NP. This problem, together with more detailed studies on the emission properties of the compound, will be tackled in a future publication.

4. Summary and conclusions

The analysis of the stability of two conformers of the thioxanthone molecule and of the electronic properties of the system by quantum-chemical methods has led us to propose a dynamical model of its structure. Planar and non-planar geometries proved to differ by less than 1 kcal/mol in stability at the MP2/6-31G(d) level of calculation, both related by a low-frequency out-of-plane mode corresponding to a "butterfly like movement" inducing the bending of the benzene rings and the out-of-plane motion of the C=O double bond. On the other hand, the comparison of CASPT2/ANO computed and experimental ionization potentials and absorption maxima and intensities of the electronic spectrum indicates that the observed features are better explained when contributions of both planar and non-planar structures are taken into account, in a dynamical model which we have named "butterfly like motion". The participation of the different conformers in the excited state dynamics will have important consequences in the photophysics of the system. As well as the proximity effect and the coupling of the nearby $\pi\pi^*$ and $n\pi^*$ excited singlet states can be claimed to explain the fluorescence quenching in non-polar environments, it is possible to envisage a model based on the conical intersection concept in which the system, after populating the $\pi\pi^*$ state and switching or not to the $n\pi^*$ state, decays by a fast internal conversion to the ground state. The relaxation would take place through a crossing seam between the lowest singlet excited and the ground state, a crossing which would be less accessible in polar solvents. The dynamic behavior of the states will change in solvated media, with effects which should be considered explicitly by proper theoretical models including both bulk and specific solvent–molecule interactions. Further studies are being carried out in which the emission properties of TX are studied and searching of conical intersections is undertaken in order to determine the energy decay pathways in TX and also to explain the solvatochromism of TX.

Acknowledgments

The research reported has been supported by the Swedish Science Research Council (VR), the Swedish National Supercomputer Center (NSC), and by projects CTQ2004-01739 of the Spanish MEC and GV04B-228 of the Generalitat Valenciana.

References

[1] D. Burget, P. Jacques, J. Chem. Phys. 88 (1991) 675–688.
[2] D. Burget, P. Jacques, J. Lumin. 54 (1992) 177–181.
[3] T. Lai, E.C. Lim, Chem. Phys. Lett. 73 (1980) 244–248.
[4] X. Allonas, C. Ley, C. Bibaut, P. Jacques, J.P. Fouassier, Chem. Phys. Lett. 322 (2000) 483–490.
[5] K.H. Giovanelli, J. Dehler, G. Hohlneicher, Ber. Bunsenges. Phys. Chem. 75 (1971) 857–863.
[6] S. Ishijima, M. Higashi, H. Yamagushi, J. Phys. Chem. 98 (1994) 10432–10435.
[7] B.O. Roos, K. Andersson, M.P. Fülscher, P.-A. Malmqvist, L. Serrano-Andrés, K. Pierloot, M. Merchán, Adv. Chem. Phys. 93 (1996) 219–331.
[8] L. Serrano-Andrés, M. Merchán, I. Nebot-Gil, R. Lindh, B.O. Roos, J. Chem. Phys. 98 (1993) 3151–3162.

[9] L. Serrano-Andrés, M. Merchán, in: P.v.R. Schegel, et al. (Eds.), Encyclopedia of Computational Chemistry, Wiley, Chichester, 2004.
[10] M. Merchán, L. Serrano-Andrés, in: M. Olivucci (Ed.), Computational Photochemistry, Elsevier, Amsterdam, 2005.
[11] K. Andersson, P.-A. Malmqvist, B.O. Roos, J. Chem. Phys. 96 (1992) 1218–1226.
[12] P.-A. Malmqvist, A. Rendell, B.O. Roos, J. Phys. Chem. 94 (1990) 5477–5482.
[13] P.-O. Widmark, P.-A. Malmqvist, B.O. Roos, Theor. Chim. Acta 77 (1990) 291–306.
[14] M.J. Frisch, et al., Gaussian '98, Revision A.11, Gaussian Inc., Pittsburgh, USA, 1998.
[15] K. Andersson, et al., Molcas, Version 6.0, Department of Theoretical Chemistry, University of Lund, Sweden, 2004.
[16] K. Iijima, I. Oonishi, S. Fujisawa, S. Shibata, Bull. Chem. Soc. Jpn. 60 (1987) 3887–3890.
[17] R. Sabbah, L. El-Watik, Can. J. Chem. 70 (1992) 24–28.
[18] S. Ishijima, M. Higashi, H. Yamagushi, M. Kubota, T. Kobayashi, J. Electron. Spectrosc. Relat. Phenom. 82 (1996) 71–74.
[19] W. Nakanishi, S. Hayashi, Y. Kusuayma, T. Negoro, S. Masuda, H. Mutoh, J. Org. Chem. 63 (1998) 8373–8379.
[20] T. Sugino, N. Kambe, N. Sonoda, T. Sakaguchi, K. Ohta, Chem. Phys. Lett. 251 (1996) 125–131.
[21] H. Lumbroso, J. Cure, M. Evers, Z. Naturforsch. 41A (1986) 1250–1257.
[22] K.A. Abdullah, T.J. Kemp, J. Photochem. 32 (1986) 49–57.
[23] M.P. Fülscher, L. Serrano-Andrés, B.O. Roos, J. Am. Chem. Soc. 119 (1997) 6168–6176.
[24] A.C. Borin, L. Serrano-Andrés, V. Ludwig, S. Canuto, Phys. Chem. Chem. Phys. 5 (2003) 5001–5009.